Calcif Tissue Int (2015) 96:552–564
DOI 10.1007/s00223-015-9981-9

ORIGINAL RESEARCH

Three-Dimensional Porous Gelapin–Simvastatin Scaffolds Promoted Bone Defect Healing in Rabbits

Ali Moshiri[1] · Mostafa Shahrezaee[1] · Babak Shekarchi[2] · Ahmad Oryan[3] · Kamran Azma[4]

Received: 15 December 2014 / Accepted: 3 March 2015 / Published online: 25 March 2015

Abstract Treatment of large bone defects (LBDs) is technically demanding. Tissue engineering is an option. A bioactive graft may be produced by combining tissue scaffolds and healing promotive factors in order to accelerate bone repair. We investigated the role of Simvastatin (Sim)-embedded porous Gelapin (Gel) scaffold on experimental bone healing. At first, the effectiveness of different concentrations of Gel and Sim powders was investigated in an experimentally induced femoral hole model in rabbits ($n = 6$) for 30 days. Then bone bioactive grafts were produced by combination of the effective concentrations of Gel, Sim, and Genipin. The bioimplants were subcutaneously tested in a rabbit model ($n = 9$) to determine their biocompatibility and biodegradability for 10–30 days. Finally, a large radial bone defect model was produced in rabbits ($n = 20$), and the bioimplants were inserted in the defects. The untreated and autograft-treated bone defects were served as controls. The animals were euthanized after 30 and 60 days of bone injury. The bone samples were evaluated by radiography, three-dimensional CT scan, bone densitometry, histopathology, and nano-indentation. At a concentration of 5 mg/hole, Sim closed the femoral bone holes after 30 days, while in the defect, autograft, and Gel groups, the holes were open. Both the Gel and Gel–Sim scaffolds were biocompatible and biodegradable. Subcutaneously, the Gel–Sim scaffold was replaced with the newly regenerated ectopic bone after 30 days. After implantation of the Gel–Sim scaffold in the radial bone defects, the scaffold was completely replaced with new woven bone after 30 days which was then matured and remodeled into a cortical bone after 60 days. Sixty days after bone injury, the Gel–Sim-treated defects had significantly higher bone volume, matrix mineralization, elastic modulus, and contact hardness when compared to the controls. The Gel–Sim scaffold may be a suitable option in managing LBDs.

Keywords Gelapin · Simvastatin · Bone · Healing · Tissue engineering · Regenerative medicine

Introduction

Large bone defects (LBDs) in the meaning of large tissue loss are a complicated problem in orthopedic surgery [1]. After multiple, compound, communited, gunshot, and complicated fractures, high energy trauma, burn, severe osteomyelitis, necrosis, gangrenous and infective deep ulcers, bone tumors (e.g., osteosarcoma), and several other conditions, it is often necessary to remove the diseased bone or fractured bone fragments (that have no vascular supply and cannot be used for reconstructive surgery), from the patient's body [2]. LBDs could occur if extensive amount of bony tissue is removed from the patient's body. The resulting defect should be initially stabilized and reconstructed by a bone substitute [3]. Auto- and allografts, the classic options in managing

Electronic supplementary material The online version of this article (doi:10.1007/s00223-015-9981-9) contains supplementary material, which is available to authorized users.

✉ Mostafa Shahrezaee
moshahrezaee@yahoo.com

[1] Department of Orthopedic Surgery, School of Medicine, AJA University of Medical Science, Tehran, Iran

[2] Department of Radiology, School of Medicine, AJA University of Medical Science, Tehran, Iran

[3] Department of Pathology, School of Veterinary Medicine, Shiraz University, Shiraz, Iran

[4] Physical Medicine and Rehabilitation Department, School of Medicine, AJA University of Medical Science, Tehran, Iran

LBDs, have significant limitations. Autografts require double surgery, which are time consuming, and associated with donor site morbidity, pain, and cosmetic concerns. In addition, there may not be enough autogenous tissue in the patient's body to reconstruct such LBDs [2, 4]. Compared to autografts, allografts have inferior healing capability and osteoinduction after transplantation. Despite modern screening technologies, allografts may still transfer infectious diseases such as HIV and hepatitis to the recipient patients [5]. In addition, application of allografts is associated with ethical concerns. Although classic grafts are routinely used in bone reconstructive surgery, their effectiveness on bone healing and regeneration is variable, and the outcome is difficult to predict [2].

Tissue engineering and regenerative medicine (TERM) is an option. Tissue scaffolds and healing promotive factors (HPFs) are two main categories in TERM [6]. To enhance osteoconduction, osteoinduction, osteoincorporation, and osteogenesis, a desirable bioactive scaffold should be biodegradable, biocompatible, and bio-efficient [2]. Gelatin (Gel) is a hydrolyzed form of collagen and could contribute in collagen production during bone healing [7, 8]. Gelatin has tissue-conductive properties and is able to promote tissue regeneration [9]. In addition, gelatin could be used as a delivery system for HPFs [8]. Because Gel scaffolds are biodegradable and biocompatible, when they are used as bone scaffolds, they do not interfere with tissue regeneration [2]. Simvastatin (Sim) is a member of the statin family of 3-hydroxy-3-methyl-glutaryl coenzyme A reductase inhibitors [10, 11]. This drug which is responsible in declining the cholesterol concentration is known to elicit numerous pleiotropic effects including enhancement of bone formation through anabolic and anti-catabolic mechanisms [12]. Simvastatin has been shown to increase the expression of growth factors particularly the VEGF and BMP2, which are the major regulators of angiogenesis and osteogenesis, both at in vitro and in vivo levels [13, 14]. By combining the Gel, as a biodegradable and biocompatible osteoconductive scaffold, with Sim, as a HPF, a suitable scaffold may be produced with the aiming to accelerate and improve bone healing and repair.

Given the above explanations, we designed, developed, and applied a new TERM-based porous Gel–Sim scaffold for bone repair. Preliminarily, we evaluated the role of different concentration of Gel and Sim on small femoral-drilled bone holes in a rabbit model. Then we produced a new three-dimensional porous Gel–Sim scaffold based on the effective concentration of each biomaterial (Gel and Sim). Consequently, we tested the subcutaneous biocompatibility and biodegradability of the scaffold and finally applied such scaffold in an experimentally induced large radial bone defect (LRBD) model in rabbits.

We hypothesized that the Gel may be a biocompatible and biodegradable material, possibly being able to enhance osteoconduction during bone healing. In addition, the porous Gel scaffold may be a suitable biomaterial for Sim delivery. After application of the Gel scaffold in LRBDs, due to the role of Gel on osteoconduction and lack of its osteoinductive properties, the Gel scaffold would probably be replaced with a new dense connective tissue (DCT) having low degree of matrix calcification. Sim may be a biocompatible and biodegradable material in vivo. Due to the beneficial roles of Sim on bone repair, controlled release of Sim from Gel scaffold may be an effective approach to enhance healing of LRBDs. If the Gel be an osteoconductive agent and Sim be an osteoinductive agent, then the Gel–Sim scaffold should induce osteogenesis by accelerating and enhancing osteoblast activity, matrix calcification, osteon formation, and new bone formation. The potential role of Sim on osteoclasts is not clear. We think that osteoclastic reaction is a part of bone remodeling, and if Sim is effective during bone repair, it should not totally inhibit osteoclastic reaction. Alternatively, it may modulate the osteoclastic reaction.

Materials and Methods

Femoral Bone Drill-hole Model

The osteoconduction, osteoinduction, and osteogenic properties of materials used to produce different bioimplants were tested in an experimentally induced femoral bone holes in rabbits. Twelve femurs in six mature male white New Zealand rabbits (body weight = 3–3.5 kg) were randomized into four equal groups (each had three femurs). Five equal femoral holes [transverse diameter (TD) = 3 mm; depth = 1.5 mm] were drilled (150 RPM) onto the lateral cortex of each femur. In the control groups, the holes were either left intact (defect) or filled with autograft powder. In the test groups, the holes were treated with different concentrations (0.25, 0.5, 1, 2, and 5 mg/hole) of Gel or Sim powder. To avoid dispersion of the applied materials and to maintain the powder within the bone cavity, an absorbable, hydrolyzed, and lyophilized collagen sponge (Technew-Cod. ANVISA No. 80015520006) was used as a plug. The muscles, subcutaneous fascia, and skin were then approximated in a routine fashion. The healing holes were harvested from the animals after 30 days and evaluated by radiology, CT scan, and histopathology.

Determination of the Effective Concentration of Gel and Sim Biomaterials

The bulk size of the femoral hole was 10.6 mm^3. The effective concentration for Gel and Sim was found to be 1 and 5 mg/hole, respectively. To produce a standard radial bone bioimplant, the effective concentration was reported as a percentage of the hole. The effective concentration of Gel and Sim which were used for fabrication of each bioimplant was 9.53 and 53 %/femoral hole bulk size, respectively. The dimensions of each bioimplants were $4 \times 4 \times 20$ mm^3 (bulk size 320 mm^3) which was almost equal to the dimensions of the radial bone defect model and was 30.18 times greater than the bulk size of the femoral bone drill-holes. The composition of the designed bioimplants for reconstruction of radial bone defects was estimated by measuring their dry weight. The dry weight of the Gel and Gel–Sim bioimplants (bulk size of each = 320 mm^3) was 30.50 mg (30.50 mg Gel) and 200.1 mg (30.50 mg Gel, 169.6 mg Sim), respectively.

Scaffold Preparation

9.53 % (95.3 mg/mL) gelatin solution (GS) (Type B; Bovine skin type; Sigma Aldrich) was prepared by dissolving the gelatin powder in deionized water (DW) at 40 °C by stirring at 100 RPM. 25 mL of the prepared GS was pipetted into a 25-mL costume made rectangular dish. To produce a Gel–Sim scaffold, 53 % (w/v) Sim (Simvastatin powder, Merck) was added to the GS and homogenized. Under shaking and stirring (100 RPM), the GS and Gel–Sim composite suspension were refrigerated at 4 °C overnight to form as gel. The Gel and Gel composites were then slowly frozen at −15 °C overnight, −20 °C for 4 h, and −70 °C for 4 h. The frozen gel composites were lyophilized for 24 h to obtain the porous sponges [8]. The lyophilized gel was cross-linked up to 90 % at room temperature (RT) in 24.4 % (w/w) Genipin (Challenge Bioproducts, Taiwan) solution [7]. After the Gel or Gel composite scaffolds were dried at RT, they were cut into several pieces of the same size and shape as the rabbit radial bone (dimensions = $4 \times 4 \times 20$ mm^3). The bioimplants were sterilized under ^{60}Co γ-irradiation (15 kGy) and suspended in ethanol (96 %) to preserve the sterility until surgical implantation [15].

Characteristics of the Scaffolds

The scaffolds ($n = 10$) were tested by scanning electron microscopy, and their porosity and pore size were measured [16, 17]. To determine the in vitro degradation behavior of the cross-linked and non-cross-linked scaffolds, the fully dehydrated scaffolds were weighed (X) and submerged in PBS in a falcon tube. After 1–10 days, the samples were washed with DW and dried on filter paper before freeze-drying. The final mass was recorded (Y) and used to calculate the percentage weight loss: weight loss (%) = $\{(X - Y)/X\} \times 100$.

The in vitro release of simvastatin in simulated body fluid (SBF) was evaluated by measuring the excitation of simvastatin at a wavelength of 238.5 nm via UV–Vis spectroscopy (Shimadzu UV-2550 Tokyo, Japan) [18]. The concentration was calculated with reference to standards prepared fresh for each analysis. The experimental setup was based on a shaking water bath (Personal-11; TAITEC Co., Tokyo, Japan) at 37 °C with a shaking rate of 180/min. One scaffold was placed in each glass vial suspended in 5 mL SBF buffer solution. The solvent was daily extracted and replaced with fresh buffer solution from day 1 to 10. The drug delivery was reported as percentage of the released drug per day.

Subcutaneous Tests

The subcutaneous biocompatibility and biodegradability of the Gel ($n = 27$) and Gel–Sim scaffolds ($n = 27$) were tested in nine white New Zealand rabbits for 10, 20, and 30 days. Under aseptic condition, six longitudinal skin incisions were made on six different areas of the dorsum back. The implants were inserted between the skin and the subcutaneous fascia, and the incisions were closed by X mattress sutures. Histologic sections were then provided from the samples after 10, 20, and 30 days of implantation.

Large Radial Bone Defect Model

The effectiveness of Gel and Gel–Sim scaffolds on healing of the experimentally induced LRBD model was tested in rabbits. Forty radial bones in twenty mature male white New Zealand rabbits were randomized into four groups (each had 10 LRBD). In the control groups, the defects were either left untreated or treated with autograft. In the test groups, the defects were either treated with Gel or Gel–Sim bioimplants. The healing radial bones were harvested after 30 and 60 days of injury.

Surgical Intervention

The animals were premedicated and anesthetized by intramuscular administration of 1 mg/kg Acepromazine maleate and 60 mg/kg Ketamine + 1 mg/kg Xylazine HCl (Alfasan Co., Woerden, Netherlands), respectively [19–21]. Under aseptic condition, a dorsomedial skin incision was made over the forearm, the extensor muscles and tendons were retracted, and the radial bone was exposed. Using electrical bone saw (Strong 204 micro-motor hand piece, SAESHIN, China), 20 mm of the middle part of the

radial bone (diaphysis) together with the covering periosteum was cut (150 RPM) under saline irrigation and was removed. After inserting the bioimplants in the defect area, the extensor muscles and tendons, subcutaneous fascia, and the skin were approximated in a routine fashion [20, 21]. Post-operative analgesia and antibiotic were provided by subcutaneous administration of 10 mg/kg tramadol (Aglobal Care, Inc., Paranaque City, Philippines) and intramuscular administration of 5 mg/kg enrofloxacin (Enrofan 5 %, Erfan, Tehran, Iran) for 5 days, respectively.

Euthanasia

The animals were anesthetized by intramuscular injection of 60 mg/kg Ketamine HCl + 2 mg/kg Xylazine HCl + 1 mg/kg Acepromazine maleate (All from Alfasan Co., Woerden, Netherlands) and euthanized by intra-cardiac injection of 1 mg/kg Gallamine triethiodide (Specia Co., Paris, France) [22, 23].

Digital Radiology

Antero-posterior and lateral radiographs were taken from the specimens harvested after euthanasia after 30 and 60 days of injury [21, 24].

Three-Dimensional Micro-computed Tomography

The specimens were examined by μ-CT using an Inveon TM unit (Siemens Healthcare, Inc., PA, USA). After calibrating the optimal exposure conditions, the samples were scanned at a section thickness of 0.05 mm. Images were reconstructed, using Inveon Research Workplace software (Siemens Healthcare USA, Inc., PA, USA), to create 3-D images of the newly formed bone and gross profiles of specimens. The bone volume of the regenerated bones was calculated from the images acquired.

Bone Densitometry

Dual-energy X-ray absorptiometry (DEXA, XR-36, Norland, CT, USA) was used to measure the bone mineral density (BMD) of a 3×3 mm^2 area in the center of the radial bone defects after 30 and 60 days of surgery. The images were taken at 20 mm/s table-moving velocity at 1 mm intervals.

Histopathology and Histomorphometry

The samples were fixed in buffered formalin (10 %), decalcified in ethylene-di-amine-tetra-acetic-acid (0.5 M, 3 weeks), dehydrated in a graded series of ethanol, cleared in xylene, embedded in paraffin wax, sectioned at 5 μm, mounted on glass slides, and finally stained with hematoxylin and eosin (H&E). Using an ordinary light microscope (Olympus, Tokyo, Japan), different magnifications ranging from ×40 to ×1000 were employed to evaluate the healing tissues.

Nanoindentation Test

Bio-Micromechanical test was carried out on 100-μm-thick bone sections, using a Nano Indenter II machine (Nano Instruments Inc., Oak Ridge TN, USA) equipped with a Berkovich diamond tip. All indentation locations ($n = 20$ for each sample) were selected within each polished specimen surface in the 500 μm diameter region using the instrument's internal microscope, and the results were averaged. Indentation test was performed under displacement control according to the following protocol: a 0.05/s constant strain rate was applied to a peak of displacement of 5000 nm, followed by a 10-s holding at peak displacement to limit the viscous behavior of bone tissue, a 45-s withdrawal to 10 % of maximum displacement, a 50-s hold period for thermal drift calculation, and final withdrawal to complete unload. The measurements were performed at a relatively high peak load ($\sim$500 mN) to overcome effects related to the heterogeneity of bone tissue at the lamellar level [25]. The bone was assumed to be isotropic with a Poisson ratio of 0.3. Indentation load–displacement curves were analyzed, using Matlab R2010 (the MathWorks Inc., Natik, MA, USA). For each indent, elastic modulus and contact hardness were calculated as previously described [25–28].

Inter-tester and Intra-tester Reliability

The investigators who undertook the measurements and analyses of the results were unaware of the experimental design and grouping details. Each evaluation and measurement were performed in triplicate, and the results were averaged. For radiologic and μ-CT evaluations, three veterinary and medical radiologists evaluated the images and reported their results. For histopathologic evaluations, three pathologists evaluated the samples and reported their results. No significant differences were seen between the results of the individuals ($p > 0.05$).

Statistical Analyses

All the quantitative values were expressed as Mean ± standard deviation and were analyzed by one (one time point) and two-way ANOVA (two time points) with their subsequent Tukey's post-hoc tests. All scored values

were expressed as median (minimum–maximum) and statistically tested, using Kruskal–Wallis *H* Test. A *p* value of <0.05 was considered statistically significant.

Results

Role of Different Biomaterials on Healing of Small Bone Drill-hole Model

Based on the radiologic and CT-scan analyses performed after 30 days of injury, none of the holes that were left untreated or either treated with autograft or different concentrations of Gel were completely close. However, the holes treated with 1 mg Gel had smaller TD compared to the holes that were treated with other concentrations of Gel ($p = 0.001$). In addition, in the Sim-treated holes, only those holes that were treated with 5 mg Sim were completely close and showed a normal radiographic opacity. Other Sim-treated holes showed inferior radiographic opacity suggesting that the mineralization was not completed at that stage. In histopathologic sections, those holes that were left untreated were entirely open and the bone marrow protruded in the holes. In the autograft-treated holes, the bone edges showed some grades of proliferation but failed to reach each other to close the holes. In the Gel group, although bone edges progressed into the center of the holes, they failed to connect with each other and were not able to close the defect. In the Sim group, those holes that were treated with 5 mg Sim were completely close and a newly regenerated bony tissue filled the holes, completely. In the 5 mg Sim-treated holes, the primary osteons were completely formed, and recanalization in the new bone was observed, showing that the healing holes were in the remodeling stage of bone healing. Those femurs that were treated with either the Gel or Sim powders showed a fin-shaped exostosis so that the exostosis in the Sim group was larger and had superior opacity when compared to the Gel group (Fig. 1).

In Vitro Characteristics of the Bioscaffolds

Under SEM, the Gel scaffold showed large pores with proper interconnectivity between the pores and optimum pore density. However, embedding the Sim crystalline within the Gel scaffold significantly reduced the porosity and pore size compared to the Gel scaffold alone ($p = 0.001$ for both). The Sim crystals were homogenously distributed in all parts of the Gel–Sim scaffold. Before cross-linking with Genipin, the Gel and Gel–Sim scaffolds were degraded after 1 and 4 days, respectively. After cross-linking procedure, 100 % of the Gel scaffolds and less than 50 % of the Gel–Sim scaffolds were degraded after 10 days, respectively. In addition, the Gel–Sim scaffold released about 5 % Sim (8.48 mg Sim) in the SBF daily so that by the first 10 days, the scaffold totally released 50.6 % (85.81 mg) of its Sim content (totally 169.6 mg Sim per scaffold) into the SBF (Fig. 2).

Subcutaneous Behavior of the Bioscaffolds

The subcutaneously implanted Gel scaffold was completely degraded and replaced by a fascia-like loose areolar connective tissue (LACT) after 20 days and remodeled to a DCT after 30 days of implantation. After subcutaneous implantation of the Gel scaffold, no characteristic inflammatory reaction was seen. Unlike the Gel scaffold, the Gel–Sim

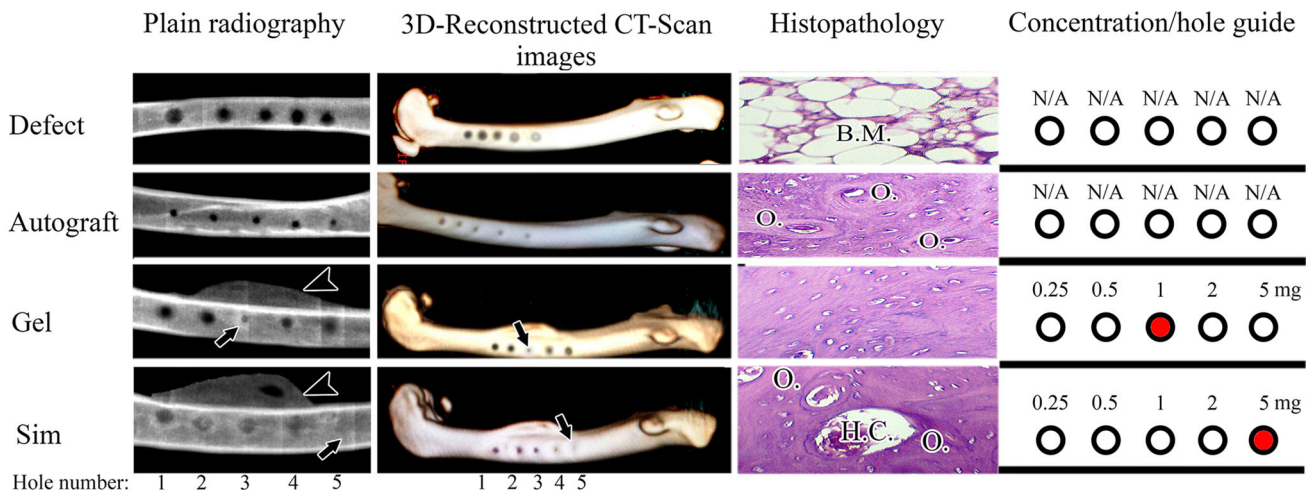

Fig. 1 Radiography (*arrows*), CT scan (*arrows*), and histologic sections (magnification = ×800) show 1 mg Gel and 5 mg Sim/hole, which are effective in the healing of bone holes. Note that Gel (1 mg) has optimum osteoconduction, while Sim (5 mg) has both osteoconductive and osteoinductive properties. *Arrows head* shows the bone exostoses regenerated on the surface of those femurs that were treated with either the Gel or Sim after 30 days. *BM* bone marrow, *O* osteon, *HC* haversian canal

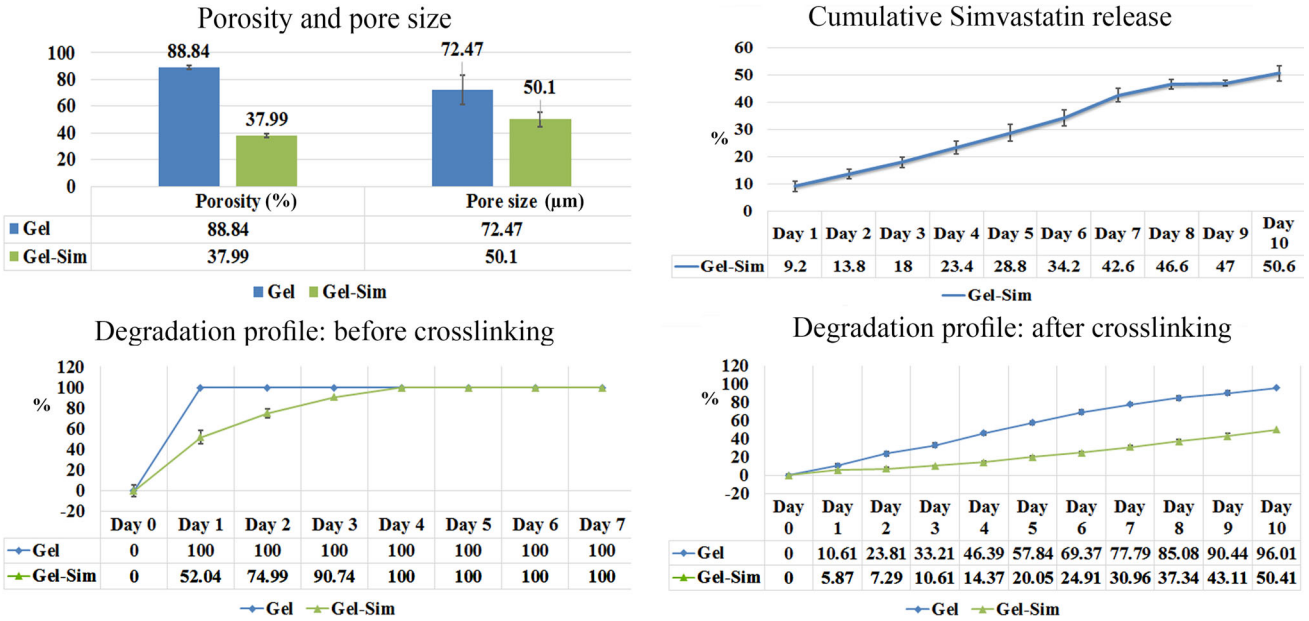

Fig. 2 In vitro characteristics of the Gel and Gel–Sim scaffolds including porosity and pore size, degradation profile, and cumulative simvastatin release pattern are presented. Note that, after embedding the Sim within the Gel scaffold, the pore size and density significantly decreased ($p > 0.05$). By cross-linking the Gel–Sim scaffold with Genipin, the degradation profile of the Gel–Sim scaffold significantly improved ($p < 0.05$) so that the cross-linked Gel–Sim scaffold continuously and homogenously released its Sim content

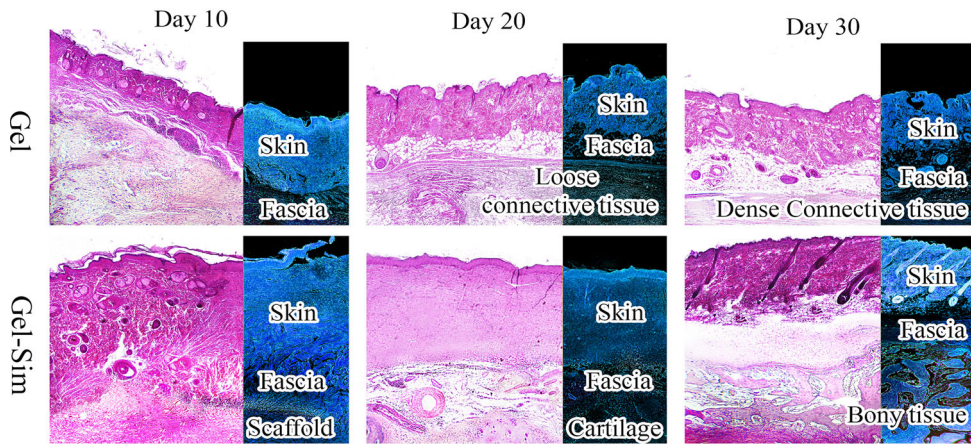

Fig. 3 After 30 days of subcutaneous implantation of the Gel and Gel–Sim scaffolds in rabbits, both types of the scaffolds were degraded and replaced by dense connective tissue and new ectopic bone-like tissue, respectively. Note that the Gel scaffold has no ability to induce osteogenesis, while the Gel–Sim scaffold is able to induce osteogenesis and is an osteoinductive scaffold

scaffold was partially degraded after ten days so that it triggered a characteristic inflammatory reaction consisting of polymorphonuclear cell infiltration and invasion of the dermis layer into the scaffold at that stage. After 20 days of Gel–Sim scaffold implantation, the inflammatory response terminated, and the scaffold was completely degraded and replaced by a cartilage-like tissue consisting of chondroblasts, collagen fibers, and large blood vessels. After 30 days, three distinct layers including skin, fascia, and newly regenerated bony matrix were detectable. In fact, the cartilaginous layer observed on day 20 developed to a woven bone on day 30, suggesting that Sim has the ability to induce ectopic new bone formation in subcutaneous area (Fig. 3).

Role of Bioscaffolds on Healing of Large Radial Bone Defect Model

Radiography, CT Scan, and Mineral Density

After 30 days of bone injury, the autograft and Gel–Sim-treated lesions showed significantly higher TD at central part of the healing tissue compared to the Gel and defect groups ($p = 0.001$). After 60 days of bone injury, the TD of the autograft-treated group significantly decreased compared to day 30 ($p = 0.001$). In addition, the Gel–Sim-treated lesions had significantly higher TD compared to the defect, autograft, and Gel groups ($p = 0.001$ for all), at 60 days of

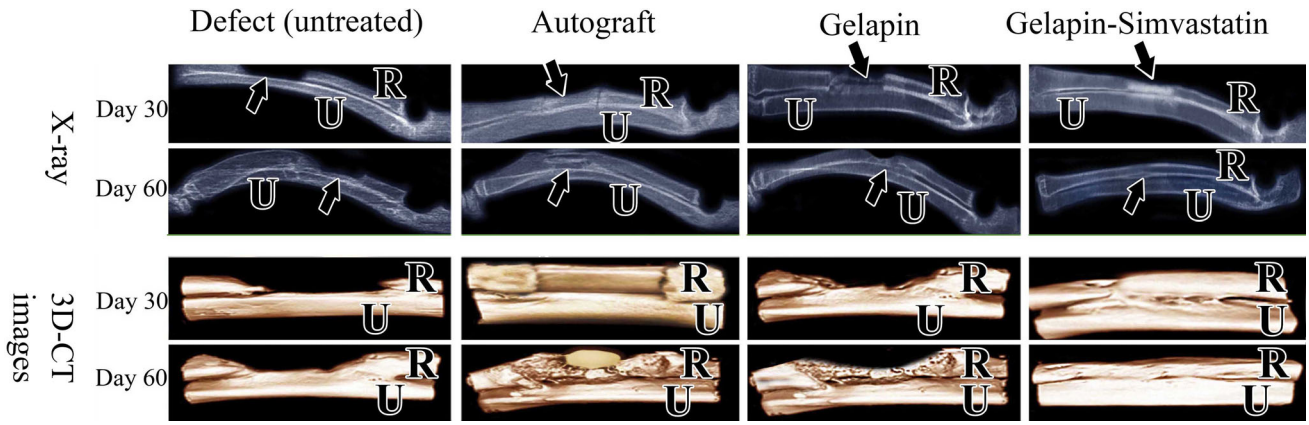

Fig. 4 Radiologic (magnification = ×1) and μ-CT scan (magnification = ×2.5) images of the defect, autograft, Gel, and Gel–Sim groups provided after 30 and 60 days of bone injury. *Arrows* show the defect area. *U* ulna, *R* radius

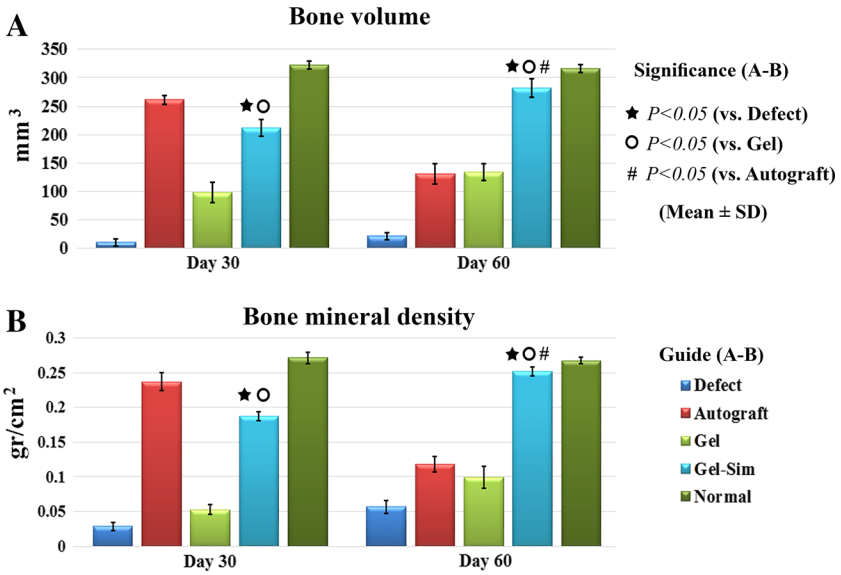

Fig. 5 Sixty days after bone injury, the Gel–Sim-treated lesions had significantly higher bone volume (**a**) and mineral density (**b**) when compared to the controls ($p = 0.001$ for all the comparisons)

injury. Thirty days after injury, due to the presence of autograft tissue in the injured area, the autograft-treated lesions had significantly higher percentage of bone filling, bone volume (Fig. 5a), and BMD (Fig. 5b) compared to the defect, Gel, and Gel–Sim groups ($p = 0.001$ for all); however, after 60 days, the autograft tissue was progressively degraded and rejected from the host and replaced by the low opacity tissue. Sixty days after bone injury, the Gel–Sim-treated lesions had significantly higher percentage bone filling, bone volume (Fig. 5a), and BMD (Fig. 5b) compared to the defect, autograft, and Gel groups ($p = 0.001$ for all) (Figs. 4, 5). After 60 days of bone injury, those lesions that were treated by Gel–Sim scaffolds showed superior scored values for bone union (2 (2–2)$^{\text{Defect}}$ vs. 1 (1–2)$^{\text{Autograft}}$ vs. 2 (1–2)$^{\text{Gelapin}}$ vs. 0 (0–0)$^{\text{Gelapin–Simvastatin}}$; $p = 0.001$), bone filling (4 (3–4)$^{\text{Defect}}$ vs. 2 (2–4)$^{\text{Autograft}}$ vs. 3 (0–4)$^{\text{Gelapin}}$ vs. 0 (0–1)$^{\text{Gelapin–Simvastatin}}$; $p = 0.001$), cortical rim formation (2 (2–2)$^{\text{Defect}}$ vs. 2 (2–2)$^{\text{Autograft}}$ vs. 2 (1–2)$^{\text{Gelapin}}$ vs. 0 (0–2)$^{\text{Gelapin–Simvastatin}}$; $p = 0.001$), callus quality (5 (5–5)$^{\text{Defect}}$ vs. 5 (4–5)$^{\text{Autograft}}$ vs. 5 (1–5)$^{\text{Gelapin}}$ vs. 0 (0–0)$^{\text{Gelapin–Simvastatin}}$; $p = 0.001$), callus homogeneity (3 (3–3)$^{\text{Defect}}$ vs. 3 (3–3)$^{\text{Autograft}}$ vs. 3 (1–3)$^{\text{Gelapin}}$ vs. 0 (0–1)$^{\text{Gelapin–Simvastatin}}$; $p = 0.001$), and medullary canal formation (2 (2–2)$^{\text{Defect}}$ vs. 2 (2–2)$^{\text{Autograft}}$ vs. 2 (2–2)$^{\text{Gelapin}}$ vs. 0 (0–1)$^{\text{Gelapin–Simvastatin}}$; $p = 0.001$) compared to the control groups ($p = 0.001$ for all) (Table S1).

Bio-micromechanical Properties

Thirty days after bone injury, the Gel–Sim-treated lesions had significantly higher elastic modulus (Fig. 6a), contact hardness (Fig. 6b), contact hardness/elastic modulus (Fig. 6c), true hardness, and total work of indentation compared to the defect and Gel groups ($p = 0.001$ for all).

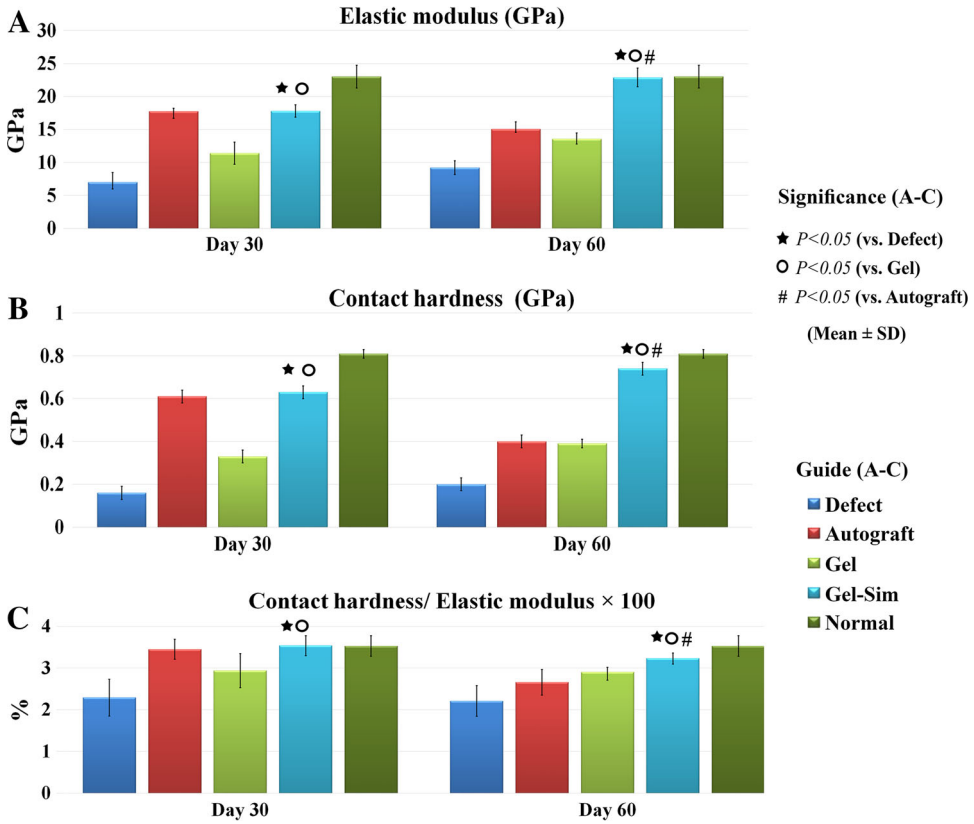

Fig. 6 Sixty days after bone injury, the Gel–Sim-treated lesions had superior bio-micromechanical properties including elastic modulus (**a**), contact hardness (**b**), contact hardness/elastic modulus (**c**) when compared to the controls ($p < 0.05$)

Due to the presence of autograft tissue in the defect area and regarding the above characteristics, there were no significant differences between the Gel–Sim-treated lesions and the autograft group at 30 days after injury ($p > 0.05$). After 60 days of bone injury, the autograft was rejected and replaced with the newly regenerated tissue. At that stage, the Gel–Sim-treated lesions had significantly higher elastic modulus (Fig. 6a), contact hardness (Fig. 6b), contact hardness/elastic modulus (Fig. 6c), true hardness, and total work of indentation compared to the defect, autograft, and Gel groups ($p = 0.001$ for all). In addition, there were no significant differences between the elastic modulus of the Gel–Sim-treated lesions with that in the normal bones at 60 days of injury ($p > 0.05$).

Histopathologic Findings

Thirty days after bone injury, no healing response was observed in the defect (no implant) group because only a LACT comparable to subcutaneous fascia filled the defect area. The fascia-like tissue composed of low density collagen fibers that haphazardly oriented throughout the defect area, immature fibroblasts, and small immature blood vessels having low TD. Sixty days after bone injury, no characteristic improvement in tissue organization was observed in the defect group so that the fascia-like tissue was still present in the defect area. Thirty days after implantation of the corticomedullary radial bone graft, the autograft was entirely present in the defect area and did not connect with the bone edges. The autograft was encapsulated by a fibrous connective tissue, but the inflammatory cells consisting of neutrophils, macrophages, and lymphocytes invaded the medullary canal of the autograft. At 60 days of bone injury, the inflammatory cells invaded the cortical parts of the autograft (compact bone) and degraded some parts of it. At that stage, the macrophages aggregated and cluster-like giant cells were seen degrading the autograft compact bone. Also, a newly regenerated tissue consisting of fibro-cartilaginous tissue filled the free spaces of the autograft tissue. These free spaces were as a result of autograft degradation. In general, sixty days after bone injury, a non-homogeneous tissue was seen in the autograft-treated lesions consisting of degraded parts of autograft tissue, fibro-cartilaginous tissue, and few parts of newly regenerated ossified tissue.

Thirty days after implantation of the Gelapin scaffold, the scaffold was totally degraded and replaced by a DCT composed of mature collagen fibers oriented in an align manner between the bone edges. In addition, the bone edges proliferated and progressed into the center of the defect area but failed to join each other. Small areas of ossification were seen in the defect area of the Gel-treated lesions. Sixty days after bone injury, the DCT observed on day 30 after injury was developed to a cartilage-like tissue in the Gel group.

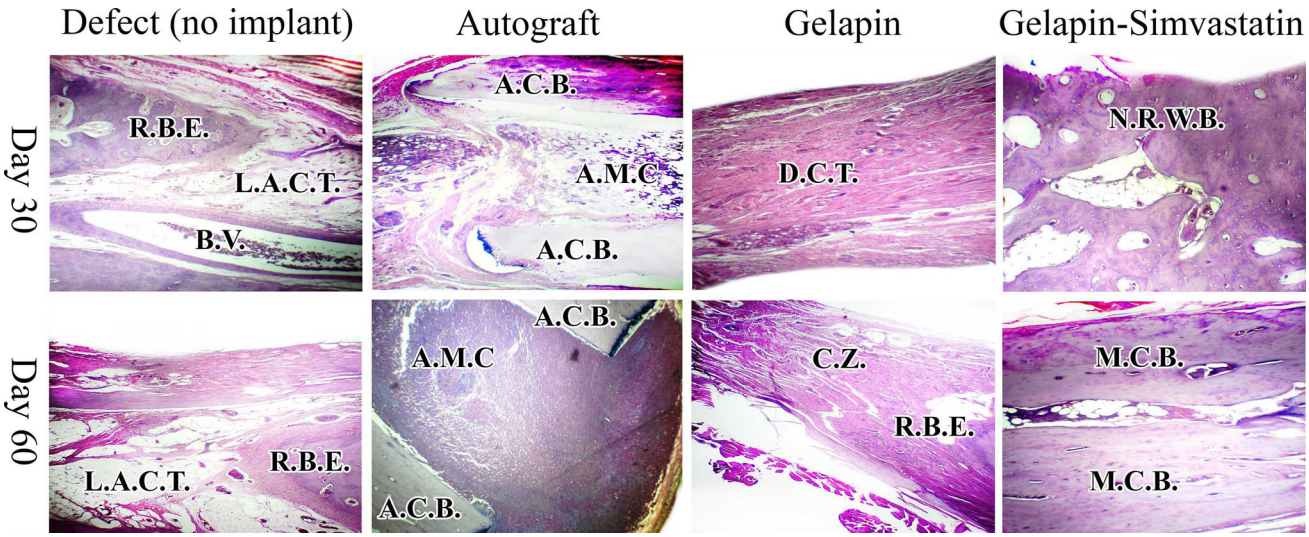

Fig. 7 Longitudinal sections obtained from the rabbit radial bones after 30 and 60 days of bone injury. Magnification = ×80. Note that actually no healing has occurred in the defect group, the autograft has been rejected in the autograft group, a fibro-cartilaginous matrix replaced the Gel scaffold in the Gel group, and finally the Gel–Sim scaffold has been replaced with the newly regenerated compact bone in the Gel–Sim group. *RBE* radial bone edge, *LACT* loose areolar connective tissue, *BV* blood vessel, *CZ* cartilaginous zone, *ACB* autograft cortical bone, *AMC* autograft medullary canal, *DCT* dense connective tissue, *NRWB* newly regenerated woven bone, *MCB* mature compact bone. Color staining *H&E*

This cartilaginous tissue was a combination of two distinct zones including hyaline cartilage and fibrocartilage. In the hyaline cartilaginous zone, few areas of endochondral ossification were observed. Thirty days after bone injury, the Gel–Sim scaffold was completely degraded and replaced by a newly regenerated woven bone consisting of osteoblasts, osteocytes, and osteoclasts. Large-sized blood vessels were seen outside of the defect area nourishing the newly regenerated woven bone in the Gel–Sim-treated lesions. Sixty days after bone injury, the woven bone developed to a compact bone tissue, and the cortex and medulla differentiated from each other. In the cortical part of the newly regenerated bone, the primary and secondary osteons were seen so that both the interstitial and circumferential lamellae developed at that stage. The osteoclasts were higher in the central part of the defect area developing the medullary canal, and both the osteoclasts and osteoblasts were present in the cortical parts developing the cortical (compact) bone. The bone marrow developed in the medullary canal of the newly regenerated bone and filled the canal. These changes resulted in formation of a newly regenerated uniform corticomedullary radial bone in the defect area connecting both the bone edges (Fig. 7).

Discussion

Both of the Gel and Sim at various concentrations/drill-hole had beneficial roles during bone healing; however, compared to different concentrations of Gel and Sim that applied in the femoral holes, the 1 mg Gel/hole and 5 mg Sim/hole had the most osteoconductive and osteoinductive properties during bone healing, respectively. The normal ability of the body failed to repair the small bone drill-holes as observed in the untreated group and the autograft powder had inferior effectiveness on bone repair compared to the 1 mg Gel and 5 mg Sim, in vivo. Based on these results, the Gel–Sim scaffold consisting of large pores with proper interconnectivity between the pores was designed. When the Gel–Sim scaffold was cross-linked by Genipin, it showed a controllable degradation profile and Sim release. After subcutaneous implantation, the Gel scaffold was rapidly absorbed and did not trigger the inflammation. The Gel scaffold was replaced by a new DCT, but due to the lack of osteoinductive properties, it failed to produce ectopic bone matrix after 30 days. In contrast, when Sim was embedded within the Gel scaffold and subcutaneously implanted in rabbits, it was degraded slower, increased inflammatory response for a short period of time, and was replaced by a cartilaginous matrix after 20 days and a newly regenerated ectopic woven bone after 30 days. In addition, Sim triggered angiogenesis and angiomaturation so that it developed the formation of large blood vessels around the ectopic bone. These beneficial effects were probably due to the role of Sim in increasing the expression of BMP-2 and VEGF [13, 14].

These results triggered us to test the bioimplants in a more clinically relevant injury model. Thus, we implanted the scaffolds in a LRBD model and evaluated their beneficial roles during bone healing. The 20 mm LRBD

produced in this experiment was about 6 times greater than the TD of the radial bone. Defects with length more than 2.5 times greater than diaphyseal TD would not heal spontaneously [2]. We also selected 30 and 60 day time points because in an effective bone healing, the hard callus forms after 4–6 weeks, while the bone healing continues by remodeling after eight to several weeks [12, 29, 30]. After insertion of the Gel–Sim scaffolds in LRBDs, the modulatory roles of Sim on inflammation, particularly the macrophages, resulted in a proper reparative phase to occur.

The osteoconductive properties of the Gel–Sim scaffold established the bone continuity which increased the mechanical weight-bearing capacity at the defect area. It also absorbed the inflammatory and regional mesenchymal cells in its architecture and did not let them to proliferate at various directions. Thus, the healing cells mostly proliferated inside the defect area so that the healing was concentrated in the injured area. The osteoinductive properties of Sim resulted in differentiation of the mesenchymal cells directly to the mature chondrocytes and osteoblasts, causing *periosteal bud* formation soon after injury. By increasing in the number of osteoblasts and osteocytes in the cortical zone, the primary osteons formed after 30 days. Unique modulatory role of Sim on osteoclasts and osteoblasts resulted in formation of the secondary osteons in the radial bone cortex, while it differentiated the medullary canal by increasing the number of osteoclasts in the medulla. The modulatory role of Sim on the activity of osteoblasts and osteoclasts is a novel finding and has not been previously reported. In fact, Sim increased new bone formation by suppressing the osteoclasts and increasing the activity of the osteoblasts at the cortical zone, while it suppressed the osteoblasts and increased the activity of the osteoclasts at the medullary zone of the hard callus. It has been shown that osteoclast suppression in response to Sim application may be the consequence of RANKL depression [29]. Formation of the secondary osteons in the Gel–Sim lesions significantly increased the elastic modulus and contact hardness of the treated bone samples when compared to the controls. Significant increase in the elastic modulus and contact hardness of the Gel–Sim-treated lesions suggests that Sim had significant roles on collagen alignment and matrix calcification which is in accordance with the histopathologic and radiologic findings.

Route of administration and duration of Sim exposure to the injured area seem to be determinant factors influencing the bone healing. In a study in rats, it has been shown that Sim administration either orally (20 mg/kg) or subcutaneously (7 mg/kg) did not improve bone repair of experimental tibial defects [30]. Alternatively, direct injection of Sim in rat bony defect for three consecutive days improved new bone formation; however, the effect did not continue when the administration was terminated [29]. Interestingly, it has been shown that oral administration of high dose Sim (120 mg/kg/daily) increased the morphology and mechanical properties of the experimentally induced femoral bone fractures in mice and rabbits [31, 32]. Although systemic administration of high dose Sim may have beneficial roles during fracture healing, this method of administration is not clinically pleasant because Sim at its high dose has side effects [31–34]. Compared to systemic methods of Sim delivery, local delivery of Sim through tissue-engineered scaffolds has this advantage that the same or even superior effects can be expected from the Sim with lower concentrations, and therefore the systemic side effects of Sim probably reduce. In addition, local delivery of Sim through tissue-engineered-based scaffolds increases the Sim exposure time to the injured area, and therefore Sim seems to effectively affect the injured area in order to promote bone healing and repair [33, 34].

Although several investigations showed that many strategies are able to accelerate bone healing and regeneration, actually most of them failed to show the remodeled bone after 8 weeks of injury [21, 35–37]. In fact, in those studies, differentiation of the cortex and medulla occurred after 12–16 weeks. We showed that controlled delivery of Sim through Gel scaffold successfully enhances bone healing so that after 8 weeks, the cortex and medulla differentiated from each other, and the new bone had almost comparable characteristics with the normal bone.

Although our implant exerted its beneficial effects during bone healing, it did not remain as a part of new bone as observed in many of the recent studies that used low biodegradable scaffolds [12, 24, 34, 35]. Zhu et al. [34] used 250 mg polylactic acid (PLA) with 50, 100, and 200 mg Sim in a LRBD model in rabbits and showed that 100 mg Sim resulted in superior bone formation compared to the controls after 16 weeks. Our investigation had the following advantages than the study of Zhu et al. [34]: first, we evaluated the role of Sim on osteoinduction, osteoconduction, and osteogenesis with or without embedding it within the Gel scaffold, in three in vivo models. Second, our sample size was larger than them. Third, we used 169.6 mg Sim in 30.50 mg Gel which was based on the results of femoral bone drill-hole model. Our bioimplant had superior porosity and biodegradability than the PLA-Sim scaffold. Finally, we showed the Gel–Sim bioimplant with 169.6 mg Sim content has superior role on bone healing when compared to the PLA-Sim with 100 mg Sim content because in our treatment strategy differentiation of the cortex and medulla and also the interstitial and circumferential lamella occurred after 8 weeks, while they showed similar results after 16 weeks. This comparison suggests that both the concentration of Sim and its carrier are important for achieving the desired effects.

Among many available biomaterials used for bone repair, only a few of them are osteoinductive. Bone morphogenetic proteins particularly the BMP-II are one of the osteoinductive compounds. However, such growth factors are expensive, require special preservative condition before surgical application, and have non-negligible limitations and side effects [38–40]. Pre-differentiated stem cells or osteoblastic cells can also induce bone formation; however, they are associated with significant limitations in the clinical situation. For instance, cell harvesting, culturing, seeding, and application require special equipment and expertise. In addition, the outcome of cell therapy is not clear because cell passaging reduces the cell life cycle, resulting in cell aging. Strontium and Bisphosphonates such as alendronate have successfully been used in preventing the osteoporosis; however, these compounds significantly reduce osteoclastogenesis which is not beneficial for bone repair [35, 41–44]. Sim is a safe agent and could controllably be released from the Gel scaffold to promote osteoinduction [10, 11, 14, 34, 45]. Future studies are appreciated if compare the role of Sim with BMPs, pre-differentiated stem cells, alendronate, and strontium in a clinically relevant animal model associated with LBDs to show which of these compounds has the most superiority in bone healing.

Although we showed that local implantation of the Gel–Sim scaffold promotes healing and regeneration of new bone in LBDs, this is an in vivo animal-based study. An animal model may closely simulate the physiological and mechanical human clinical condition, but it is only an approximation and each animal model has its unique advantages and disadvantages. Rabbit is a widely accepted animal model in studying human diseases, particularly in the fields of orthopedic surgery; however, rabbits have a different pattern for weight bearing, and this can potentially affect the radial bone healing. The age, diet, anatomic, and physiologic conditions of rabbits have some differences with humans. These limitations should be considered when the results of the present investigation are going to be translated into the clinical setting.

Conclusion

The Gel had osteoconductive properties and was a biocompatible and biodegradable biomaterial suitable for scaffold preparation and controlled drug delivery. Sim had both osteoconductive and osteoinductive properties. Application of 1 mg Gel/10.6 mm^3 and 5 mg Sim/10.6 mm^3 femoral bone drill-holes increased new bone formation significantly more than the controls. The Gel and Gel–Sim scaffolds, when subcutaneously implanted in rabbits, were replaced by a DCT and an ectopic bone matrix after 30 days, respectively. Implantation of the Gel–Sim scaffold in LRBD model in rabbits, significantly increased post-operative inflammation for a short period of time, increased osteoblasts and chondrocytes proliferation and matrix production which increased primary osteon formation after 30 days. The Gel–Sim scaffold remodeled a new callus by increasing the number of macrophages and their differentiation into the osteoclasts so that by modulating the osteoblast and osteoclast activity at the peripheral parts of the hard callus, Sim improved the development of secondary osteons and by inhibiting the osteoblast activity and increasing the osteoclast activity in the central parts of the callus, it differentiated the medullary canal from the cortex. The Gel–Sim scaffolds did not remain as a part of the new bone and were replaced by the newly regenerated corticomedullary radial bone that had superior morphology and function when compared to the controls. The Gel–Sim scaffold was biocompatible, biodegradable, and bioeffective by means of osteoconduction, osteoinduction, and osteogenesis. Such treatment strategy may be a valuable option in bone reconstructive surgery; however, more in vivo confirmation would be appreciated before its clinical application.

Acknowledgments The authors would like to thank the authorities of AJA University of Medical Sciences for providing the facilitations in performing the present investigation. The kind cooperation of Mr. A. Navideh (Department of Radiology), Mr. M. Chehri (Department of Pathology), Mr. S. Shirzadi (Animal Laboratory center), and Mr. M. Younesi (Department of Radiology, Faculty of Medicine, AJA, University of Medical Sciences, Tehran, Iran) is fully acknowledged.

Conflict of interest This is the authors' own work. Dr Ali Moshiri reports that neither conflict of interest nor financial disclosure is present associated with this work or its related contents. Dr Mostafa Shahrezaie reports that neither conflict of interest nor financial disclosure is present associated with this work or its related contents. Dr Babak Shekarchi reports that neither conflict of interest nor financial disclosure is present associated with this work or its related contents. Prof. Ahmad Oryan reports that neither conflict of interest nor financial disclosure is present associated with this work or its related contents. Dr. Kamran Azma reports that neither conflict of interest nor financial disclosure is present associated with this work or its related contents.

Human and Animal Rights and Informed Consent statement All animals received humane care in compliance with the Guide for Care and use of Laboratory Animals (NIH publication No. 85–23, revised 1985). The study was approved by the local Ethics Committee of AJA University of Medical Science.

References

1. Oryan A, Alidadi S, Moshiri A (2013) Current concerns regarding healing of bone defects. Hard Tissue 2:13. http://www.oapublishinglondon.com/article/374
2. Oryan A, Alidadi S, Moshiri A, Maffulli N (2014) Bone regenerative medicine: classic options, novel strategies, and future directions. J Orthop Surg Res 9:18

3. Moshiri A, Oryan A, Shahrezaee M (2015) An overview on bone tissue engineering and regenerative medicine: current challenges, future directions and strategies. J Sports Med Doping Stud 5:e144. doi:10.4172/2161-0673.1000e144
4. Kolk A, Handschel J, Drescher W, Rothamel D, Kloss F, Blessmann M, Heiland M, Wolff KD, Smeets R (2012) Current trends and future perspectives of bone substitute materials—from space holders to innovative biomaterials. J Craniomaxillofac Surg 40:706–718
5. Calvo R, Figueroa D, Díaz-Ledezma C, Vaisman A, Figueroa F (2011) Bone allografts and the functions of bone banks. Rev Med Chil 139:660–666
6. Moshiri A, Oryan A, Meimandi-Parizi A, Koohi-Hosseinabadi O (2014) Effectiveness of xenogenous-based bovine-derived platelet gel embedded within a three-dimensional collagen implant on the healing and regeneration of the Achilles tendon defect in rabbits. Expert Opin Biol Ther 14:1065–1089
7. Kirchmajer DM, Watson CA, Ranson M (2013) Gelapin, a degradable genipin cross-linked gelatin hydrogel. RSC Adv 3:1073–1081
8. Rodriguez IA, Sell SA, McCool JM, Saxena G, Spence AJ, Bowlin GL (2013) A preliminary evaluation of lyophilized gelatin sponges, enhanced with platelet-rich plasma, hydroxyapatite and chitin whiskers for bone regeneration. Cells 2:244–265
9. Seo JP, Tsuzuki N, Haneda S, Yamada K, Furuoka H, Tabata Y, Sasaki N (2014) Osteoinductivity of gelatin/β-tricalcium phosphate sponges loaded with different concentrations of mesenchymal stem cells and bone morphogenetic protein-2 in an equine bone defect model. Vet Res Commun 38:73–80
10. Killeen AC, Rakes PA, Schmid MJ, Zhang Y, Narayana N, Marx DB, Payne JB, Wang D, Reinhardt RA (2012) Impact of local and systemic alendronate on simvastatin-induced new bone around periodontal defects. J Periodontol 83:1463–1471
11. Jiang L, Sun H, Yuan A, Zhang K, Li D, Li C, Shi C, Li X, Gao K, Zheng C, Yang B, Sun H (2013) Enhancement of osteoinduction by continual simvastatin release from poly(lactic-co-glycolic acid)-hydroxyapatite-simvastatin nano-fibrous scaffold. J Biomed Nanotechnol 9:1921–1928
12. Pullisaar H, Tiainen H, Landin MA, Lyngstadaas SP, Haugen HJ, Reseland JE, Ostrup E (2013) Enhanced in vitro osteoblast differentiation on TiO_2 scaffold coated with alginate hydrogel containing simvastatin. J Tissue Eng 4:2041731413515670
13. Wong RWK, Rabie ABM (2003) Statin collagen grafts used to repair defects in the parietal bone of rabbits. J Oral Maxillofac Surg 41:244–248
14. Oliveira NM, Correa VB, Chavez VEA (2011) Early alveolar bone regeneration in rats after topical administration of simvastatin. Oral Surg Oral Med Oral Pathol Oral Radiol Endod 112:170–179
15. Moshiri A, Oryan A, Meimandi-Parizi A (2013) Role of tissue-engineered artificial tendon in healing of a large Achilles tendon defect model in rabbits. J Am Coll Surg 217(421–441):e8
16. Moshiri A, Oryan A, Meimandi-Parizi A, Silver IA, Tanideh N, Golestani N (2013) Effectiveness of hybridized nano- and microstructure biodegradable, biocompatible, collagen-based, three-dimensional bioimplants in repair of a large tendon-defect model in rabbits. J Tissue Eng Regen Med. doi:10.1002/term.1740
17. Meimandi-Parizi A, Oryan A, Moshiri A (2013) Tendon tissue engineering and its role on healing of the experimentally induced large tendon defect model in rabbits: a comprehensive in vivo study. PLoS ONE 8:e73016
18. Chou J, Ito T, Otsuka M, Ben-Nissan B, Milthorpe B (2013) The effectiveness of the controlled release of simvastatin from β-TCP macrosphere in the treatment of OVX mice. J Tissue Eng Regen Med. doi:10.1002/term.1784
19. Oryan A, Moshiri A, Meimandi-Parizi A (2014) Implantation of a novel tissue-engineered graft in a large tendon defect initiated inflammation, accelerated fibroplasia and improved remodeling of the new Achilles tendon: a comprehensive detailed study with new insights. Cell Tissue Res 355:59–80
20. Oryan A, Meimandi Parizi A, Shafiei-Sarvestani Z, Bigham AS (2012) Effects of combined hydroxyapatite and human platelet rich plasma on bone healing in rabbit model: radiological, macroscopical, hidtopathological and biomechanical evaluation. Cell Tissue Bank 13:639–651
21. Parizi AM, Oryan A, Shafiei-Sarvestani Z, Bigham AS (2012) Human platelet rich plasma plus Persian Gulf coral effects on experimental bone healing in rabbit model: radiological, histological, macroscopical and biomechanical evaluation. J Mater Sci Mater Med 23:473–483
22. Oryan A, Moshiri A, Meimandi-Parizi A (2014) In vitro characterization of a novel tissue engineered based hybridized nano and micro structured collagen implant and its in vivo role on tenoinduction, tenoconduction, tenogenesis and tenointegration. J Mater Sci Mater Med 25:873–897
23. Oryan A, Moshiri A, Parizi AM, Maffulli N (2014) Implantation of a novel biologic and hybridized tissue engineered bioimplant in large tendon defect: an in vivo investigation. Tissue Eng Part A 20:447–465
24. Shafiei-Sarvestani Z, Oryan A, Bigham AS, Meimandi-Parizi A (2012) The effect of hydroxyapatite-hPRP, and coral-hPRP on bone healing in rabbits: radiological, biomechanical, macroscopic and histopathologic evaluation. Int J Surg 10:96–101
25. Oliver WC, Pharr GM (1992) An improved technique for determining hardness and elastic modulus. J Mater Res 7:1564–1583
26. Sakai M (1999) The Meyer Hardness: a measure for plasticity? J Mater Res 14:3630–3639
27. Oyen ML (2006) Nanoindentation hardness of mineralized tissues. J Biomech 39:2699–2702
28. Bala Y, Depalle B, Douillard T, Meille S, Clément P, Follet H, J Chevalier, Boivin G (2011) Respective roles of organic and mineral components of human cortical bone matrix in micromechanical behavior: an instrumented study. J Mech Behav Biomed Mater 4:1473–1482
29. Ayukawa Y, Yasukawa E, Moriyama Y, Ogino Y, Wada H, Atsuta I, Koyano K (2009) Local application of statin promotes bone repair through the suppression of osteoclasts and the enhancement of osteoblasts at bone-healing sites in rats. Oral Surg Oral Med Oral Pathol Oral Radiol Endod 107:336–342
30. Anbinder AL, Junqueira JC, Mancini MN, Balducci I, Rocha RF, Carvalho YR (2006) Influence of simvastatin on bone regeneration of tibial defects and blood cholesterol level in rats. Braz Dent J 17:267–273
31. Skoglund B, Forslund C, Aspenberg P (2002) Simvastatin improves fracture healing in mice. J Bone Miner Res 17:2004–2008
32. Saraf SK, Singh A, Garbyal RS, Singh V (2007) Effect of simvastatin on fracture healing–an experimental study. Indian J Exp Biol 45:444–449
33. Thylin MR, McConnell JC, Schmid MJ, Reckling RR, Ojha J, Bhattacharyya I, Marx DB, Reinhardt RA (2002) Effects of simvastatin gels on murine calvarial bone. J Periodontol 73:1141–1148
34. Zhu J, Song Q, Wang J, Han X, Yang Y, Liao J, Song C (2010) Study on local implantation of simvastatin for repairing rabbit radial critical size defects. Zhongguo Xiu Fu Chong Jian Wai Ke Za Zhi 24:465–471
35. Chen J, Luo Y, Hong L, Ling Y, Pang J, Fang Y, Wei K, Gao X (2011) Synthesis, characterization and osteoconductivity properties of bone fillers based on alendronate-loaded poly(ε-caprolactone)/hydroxyapatite microspheres. J Mater Sci Mater Med 22:547–555

36. Ni M, Li G, Tang PF, Chan KM, Wang Y (2011) rhBMP-2 not alendronate combined with HA-TCP biomaterial and distraction osteogenesis enhance bone formation. Arch Orthop Trauma Surg 131:1469–1476
37. Wu Y, Hou J, Yin M, Wang J, Liu C (2014) Enhanced healing of rabbit segmental radius defects with surface-coated calcium phosphate cement/bone morphogenetic protein-2 scaffolds. Mater Sci Eng C Mater Biol Appl 44:326–335
38. Zhou P, Xia Y, Cheng X, Wang P, Xie Y, Xu S (2014) Enhanced bone tissue regeneration by antibacterial and osteoinductive silica-HACC-zein composite scaffolds loaded with rhBMP-2. Biomaterials 35:10033–10045
39. Cao L, Wang J, Hou J, Xing W, Liu C (2014) Vascularization and bone regeneration in a critical sized defect using 2-N,6-O-sulfated chitosan nanoparticles incorporating BMP-2. Biomaterials 35:684–698
40. Oryan A, Alidadi S, Moshiri A, Bigham-Sadegh A (2014) Bone morphogenetic proteins: a powerful osteoinductive compound with non-negligible side effects and limitations. BioFactors 40:459–481
41. Boanini E, Torricelli P, Gazzano M, Della Bella E, Fini M, Bigi A (2014) Combined effect of strontium and zoledronate on hydroxyapatite structure and bone cell responses. Biomaterials 35:5619–5626
42. Fernández JM, Molinuevo MS, McCarthy AD, Cortizo AM (2014) Strontium ranelate stimulates the activity of bone-specific alkaline phosphatase: interaction with Zn(2+) and Mg (2+). Biometals 27:601–607
43. Li Y, Luo E, Zhu S, Li J, Zhang L, Hu J (2014) Cancellous bone response to strontium-doped hydroxyapatite in osteoporotic rats. J Appl Biomater Funct Mater. doi:10.5301/jabfm.5000168
44. Lima H, Maia J, Bandeira F (2014) Trajectories of bone remodeling markers and bone mineral density during treatment with Strontium Ranelate in postmenopausal women previously treated with bisphosphonates. Clin Med Insights Endocrinol Diabetes 7:7–11
45. Rojbani H, Nyan M, Ohya K, Kasugai S (2011) Evaluation of the osteoconductivity of α-tricalcium phosphate, β-tricalcium phosphate, and hydroxyapatite combined with or without simvastatin in rat calvarial defect. J Biomed Mater Res A 98:488–498